Early alterations in stem-like/marrow-resident T cells and innate and myeloid cells in preneoplastic gammopathy

Jithendra Kini Bailur,[1] Samuel S. McCachren,[1,2] Deon B. Doxie,[1] Mahesh Shrestha,[1] Katherine Pendleton,[1] Ajay K. Nooka,[1,3] Natalia Neparidze,[4] Terri L. Parker,[4] Noffar Bar,[4] Jonathan L. Kaufman,[1,3] Craig C. Hofmeister,[1,3] Lawrence H. Boise,[1,3] Sagar Lonial,[1,3] Melissa L. Kemp,[2] Kavita M. Dhodapkar,[3,5] and Madhav V. Dhodapkar[1,3]

[1]Department of Hematology/Oncology, Emory University School of Medicine, Atlanta, Georgia, USA. [2]The Wallace H. Coulter Department of Biomedical Engineering, Georgia Institute of Technology and Emory University, Atlanta, Georgia, USA. [3]Winship Cancer Institute, Atlanta, Georgia, USA. [4]Section of Hematology, Yale University School of Medicine, New Haven, Connecticut, USA. [5]Department of Pediatrics, Children's Healthcare of Atlanta, Emory University, Atlanta, Georgia, USA.

Preneoplastic lesions carry many of the antigenic targets found in cancer cells but often exhibit prolonged dormancy. Understanding how the host response to premalignancy is maintained and altered during malignant transformation is needed to prevent cancer. To understand the immune microenvironment in precursor monoclonal gammopathy of undetermined significance (MGUS) and myeloma, we analyzed bone marrow immune cells from 12 healthy donors and 26 patients with MGUS/myeloma by mass cytometry and concurrently profiled transcriptomes of 42,606 single immune cells from these bone marrow samples. Compared with age-matched healthy donors, memory T cells from both MGUS and myeloma patients exhibited greater terminal effector differentiation. However, memory T cells in MGUS show greater enrichment of stem-like TCF1/7^{hi} cells. Clusters of T cells with stem-like and tissue residence genes were also found to be enriched in MGUS by single-cell transcriptome analysis. Early changes in both NK and myeloid cells were also observed in MGUS. Enrichment of stem-like T cells correlated with a distinct genomic profile of myeloid cells and levels of Dickkopf-1 in bone marrow plasma. These data describe the landscape of changes in both innate and adaptive immunity in premalignancy and suggest that attrition of the bone marrow–resident T cell compartment because of loss of stem-like cells may underlie loss of immune surveillance in myeloma.

Introduction

Most human cancers are preceded by a long phase of premalignant lesions that are more common than the cancer itself. Multiple myeloma (MM) is a common hematologic malignancy wherein tumor cells grow predominantly in the bone marrow. All cases of MM are preceded by a precursor state termed as monoclonal gammopathy of undetermined significance (MGUS) (1). MGUS/MM is an attractive model to gain basic insights into early host response in human cancer because the precursor state is unresectable. Studies in mouse models have illustrated the capacity of the immune system to prevent, edit, or sculpt early tumors, mediated at least in part by T cell recognition of neoantigens. In the setting of cancer, T cell exhaustion as well as other immune-suppressive cells inhibit tumor immunity. However, because many neoantigens originate early during carcinogenesis, precisely when during carcinogenesis such exhaustion programs emerge and how these exhausted clones are maintained in human cancer/pre-cancer remain to be elucidated. Tumor cells in MGUS carry the great majority of genomic alterations, including the mutational burden found in MM (2). Prior studies have demonstrated the capacity of T cells to mediate specific recognition of MGUS cells (3, 4); recent data also show alterations in innate lymphoid cells in these lesions (5). Antitumor T cells are often enriched in the bone marrow of MM patients (6, 7); therapeutic adoptive transfer of bone marrow T cells is being explored in MM (8). Recent prospective studies have shown that host immune response in MGUS can predict the risk of malignant

transformation (9). Data from humanized mouse models also suggest that dormancy of MGUS lesions is controlled by tumor-extrinsic factors (10). Therefore, understanding the biology of immune cells infiltrating MGUS lesions may provide valuable insights into pathogenesis of MM.

One deficiency of existing studies is that only limited information on cell states and phenotypes of individual cells in the tumor microenvironment was obtained. To overcome these limitations, we performed high-dimensional single-cell RNA-sequencing (scRNA-Seq) and mass cytometry analysis on immune cells in the MGUS/MM bone marrow microenvironment to gain deeper insights into these cells, both at transcriptomic as well as proteomic level. We focused on the nontumor compartment in both MM and MGUS and performed comparisons with immune cells in bone marrow from healthy donors.

Results

To analyze immune cells in the bone marrow in MGUS/MM, we analyzed bone marrow mononuclear cells by mass cytometry using 57 markers (clinical characteristics in Supplemental Table 1, mass cytometry panel in Supplemental Table 2; supplemental material available online with this article; https://doi.org/10.1172/jci.insight.127807DS1). In view of the importance of CD8$^+$ memory T cells in tumor immunity, we first examined the CD8$^+$ memory T cell compartment, which revealed a modest decline in CD8$^+$ central memory T cells (Tcms) in MM (Figure 1A). MM had a slightly higher proportion of CD8$^+$ effector/effector memory T cells (Tems + terminal effectors [Ttes]) (Figure 1B). However, the proportion of Ttes expressing high levels of granzyme B was significantly increased in both MGUS and MM compared with age-matched healthy donors (Figure 1, C and D, and Supplemental Figure 1).

To better characterize these changes in effector differentiation, we analyzed the expression of several T cell–associated transcription factors in memory T cells. Of these, the expression of T cell factor 1 (TCF1) was significantly increased among memory CD8$^+$ T cells in the MGUS cohort, while the expression of T-bet, Eomes, and GATA-3 did not differ (Figure 1, E and F). A similar trend for increase in TCF1 expression was seen among CD4$^+$ memory T cells in MGUS (Supplemental Figure 2A). The proportions of CD4$^+$ T cells expressing Eomes and T-bet were also significantly lower in MGUS and MM cohorts (Supplemental Figure 2B). Together these data show that even though T cells infiltrating both MM and MGUS have enhanced effector differentiation, there are distinct differences in transcription factor expression in these cells.

Observed differences in the expression of TCF1 in premalignancy were of particular interest because of its emerging role in regulating T cell stemness in memory CD8$^+$ T cells during chronic infections and possibly cancer (11–14). TCF1 expression in human T cells follows a distinct gradient, with stem-like features associated with TCF1^{hi}T-bet^{lo} cells (14). Using a similar gating strategy (Figure 1G), the proportion of TCF1^{hi} cells was found to be significantly increased in MGUS, while TCF1$^-$ cells were higher in MM (Figure 1H). The increase in TCF1^{hi} CD8$^+$ T cells in MGUS was observed in both Tcm and Tem compartments (Figure 1I). TCF1^{hi} cells in all 3 patient cohorts had a distinct phenotype, with increased expression of CD127, CD27, and CXCR4 (marker of bone marrow homing), as well as reduced expression of T-bet, Eomes, and lytic genes, such as granzyme B (Figure 1J). Thus, CD8$^+$ memory T cells infiltrating MGUS lesions are particularly enriched for phenotypes associated with enhanced stemness.

Analysis of the myeloid compartment (gating strategy in Supplemental Figure 3) was performed to identify markers differentially expressed between myeloid cells infiltrating MGUS and MM. These studies identified a decline in the expression of CD95, CD86, c-KIT, and CD155 and an increase in programmed death ligand 1 (PD-L1) expression on myeloid cells in MM compared with healthy donors, while there were no differences in other markers, such as HLA-DR (Figure 2, A and B). We identified 3 distinct clusters of myeloid cells based on the expression of CD14 and CD11b, with MGUS/MM lesions enriched in the proportion of CD14$^-$CD11b$^+$ myeloid cells (Supplemental Figure 4). Analysis of NK cells revealed a slight increase in total NK cells in MM; subsequent analysis of the CD56^{lo} NK subset revealed a decline in natural killer group 2, member D (NKG2D) expression in MM (Supplemental Figure 4). Thus, alterations in innate myeloid and NK cells originate early in myelomagenesis.

scRNA-Seq of CD138-depleted cells from MM, as well as total bone marrow mononuclear cells from healthy donors or patients with MGUS, was performed to further analyze the heterogeneity of immune cells in the bone marrow of these cohorts. After excluding plasma cells and low-quality cells, k-nearest neighbor unsupervised clustering of 42,606 cells (9840 cells from healthy donors, 20,286 cells from MGUS, 12,480 cells from MM) created a detailed map comprising 15 transcriptionally distinct subpopulations, which were also aligned to distinct cell types (Figure 3, A and B, and Supplemental Tables 3 and 4). Several of these clusters were differen-
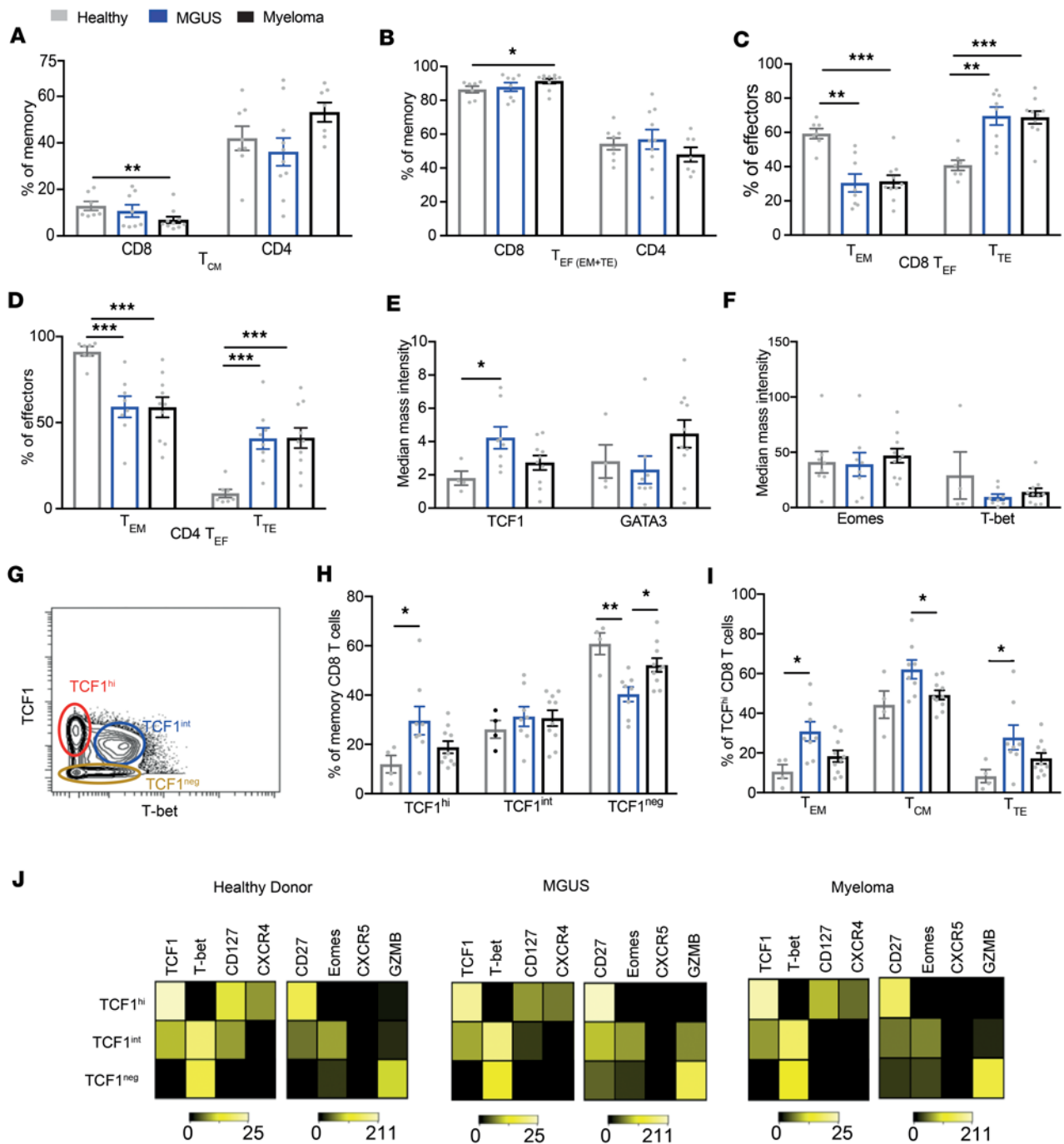
Figure 1. Bone marrow mononuclear cells from healthy donors (*n* = 7), MGUS (*n* = 8), and myeloma (*n* = 10) were characterized using single-cell mass cytometry. (**A**) Central memory (CD45RO⁺CCR7⁺) CD8⁺ and CD4⁺ T cells as percentage of total memory CD8⁺ and CD4⁺ T cells. (**B**) CD8⁺ and CD4⁺ effector T cells (Tefs) (effector memory cells, Tems: CD45RO⁺CCR7⁻; and terminal effectors, Ttes: CD45RO⁻CCR7⁻) as percentage of total memory CD8⁺ and CD4⁺ T cells. (**C**) CD8⁺ Tems and Ttes as percentage of CD8⁺ Tefs. (**D**) CD4⁺ Tems and Ttes as percentage of CD4⁺ Tefs. (**E**) Median expression of TCF1 and GATA-3 transcription factors in CD8⁺ memory T cells. (**F**) Median expression of Eomes and T-bet in memory CD8⁺ T cells. (**G**) Gating strategy for defining cells that express high levels of TCF1 (TCF¹ʰⁱ) and intermediate levels of TCF1 (TCF¹ⁱⁿᵗ) and those that do not express TCF1 transcription factor (TCF¹ⁿᵉᵍ). A representative dot plot from a patient with MGUS. (**H**) Percentage of memory CD8⁺ T cells that express TCF1ʰⁱ or TCF¹ⁿᵗ or lack TCF1 expression (TCF¹ⁿᵉᵍ). (**I**) Percentage of TCF1ʰⁱ in CD8⁺ Tems, Tcms, and Ttes. (**J**) Characteristics of the TCF1ʰⁱ, TCF1ⁱⁿᵗ, and TCF1ⁿᵉᵍ CD8⁺ memory T cells. All bar graphs show mean ± SEM. *$P <$ 0.05, **$P <$ 0.01, ***$P <$ 0.001, Mann-Whitney test.
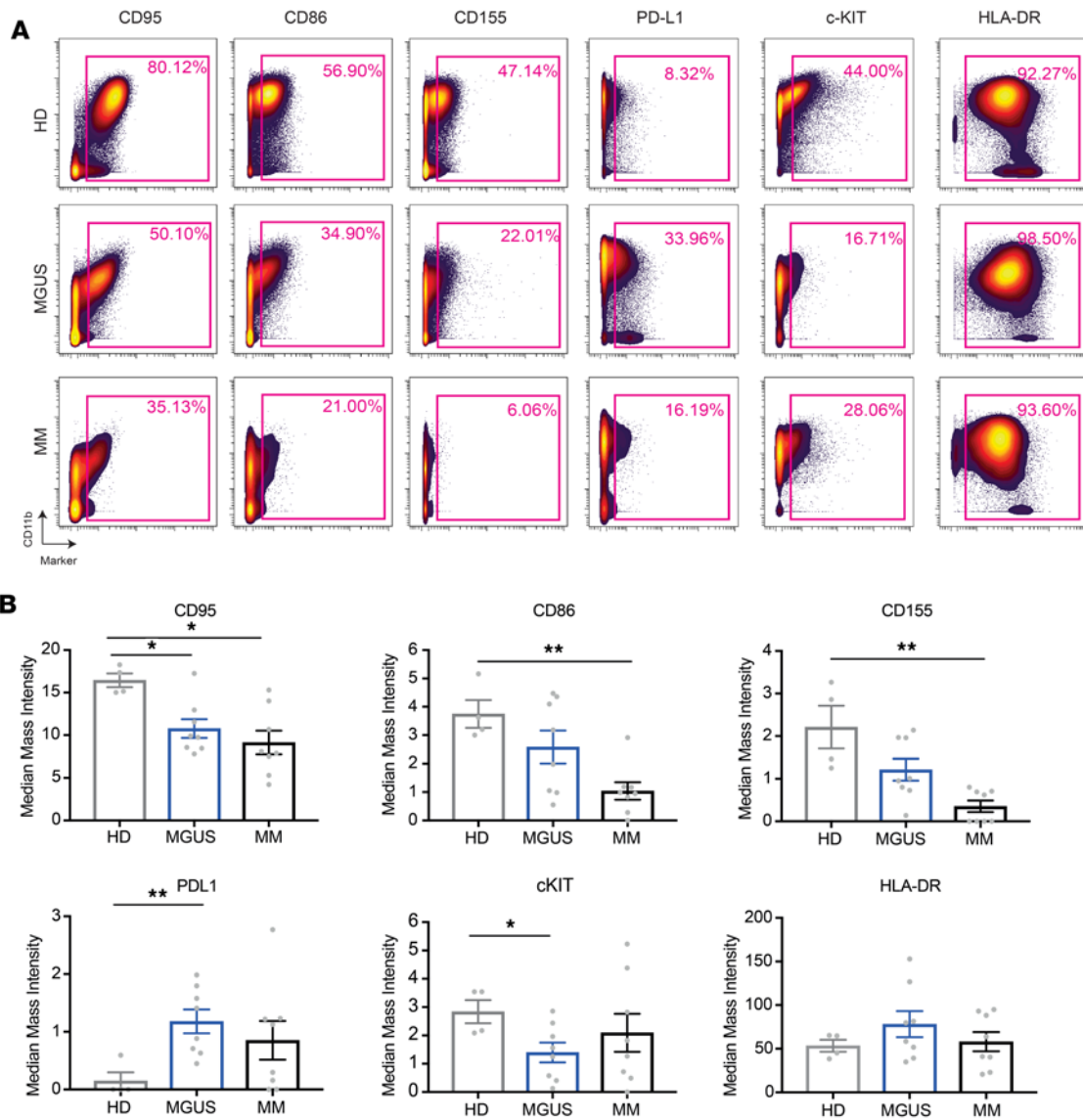
Figure 2. Bone marrow myeloid cells were identified using single-cell mass cytometry analysis of bone marrow mononuclear cells from healthy donors (*n* = 4), MGUS (*n* = 8), and myeloma (*n* = 8) (gray, blue, and black, respectively). Gating strategy of myeloid cells is described within Supplemental Figure 3. (**A**) Biaxial plots of CD11b versus CD95, CD86, CD155, PD-L1, c-KIT, and HLA-DR of healthy, MGUS, and myeloma donor myeloid cells. (**B**) Bulk myeloid cells' median intensity for CD95, CD86, CD155, PD-L1, c-KIT, and HLA-DR. All bar graphs show mean ± SEM. *$P < 0.05$, **$P < 0.01$.

tially represented between the 3 cohorts (Figure 3, C and D). Analysis of immune composition by scRNA-Seq correlated with mass cytometry data; for example, the decline in B cells in MM by mass cytometry was also reflected in the decline in major B cell cluster (B1) in MM (Supplemental Figure 5 and Figure 3D).

The most notable differences between T cells in MGUS and MM related to 2 distinct T cell clusters (clusters T2 and T3) (Figure 4A). T2 cluster (overrepresented in MGUS and reduced in MM) was characterized by increased expression of stem-like genes (TCF1/TCF7) consistent with data from mass cytometry, as well as genes associated with tissue residence (NR4A2, CD69) (15, 16) and reduced expression of lytic genes (granzyme A, granzyme K). In contrast, T3 cluster (increased in MM) was characterized by the expression of lytic genes (e.g., granzyme A), senescence-associated genes (e.g., KLRG1), and proinflammatory cytokines (e.g., IL-32) (Figure 4B). Gene set enrichment analysis (GSEA) of these genes identified pathways related to effector functions and programmed cell death 1–mediated (PD-1–mediated) exhaustion programs as key pathways distinguishing MM-enriched clusters (Supplemental Figure 6). T2 cluster, enriched in MGUS, was also enriched for pathways associated with stem cell memory cells (Supplemental Figure 6) as mass cytome-
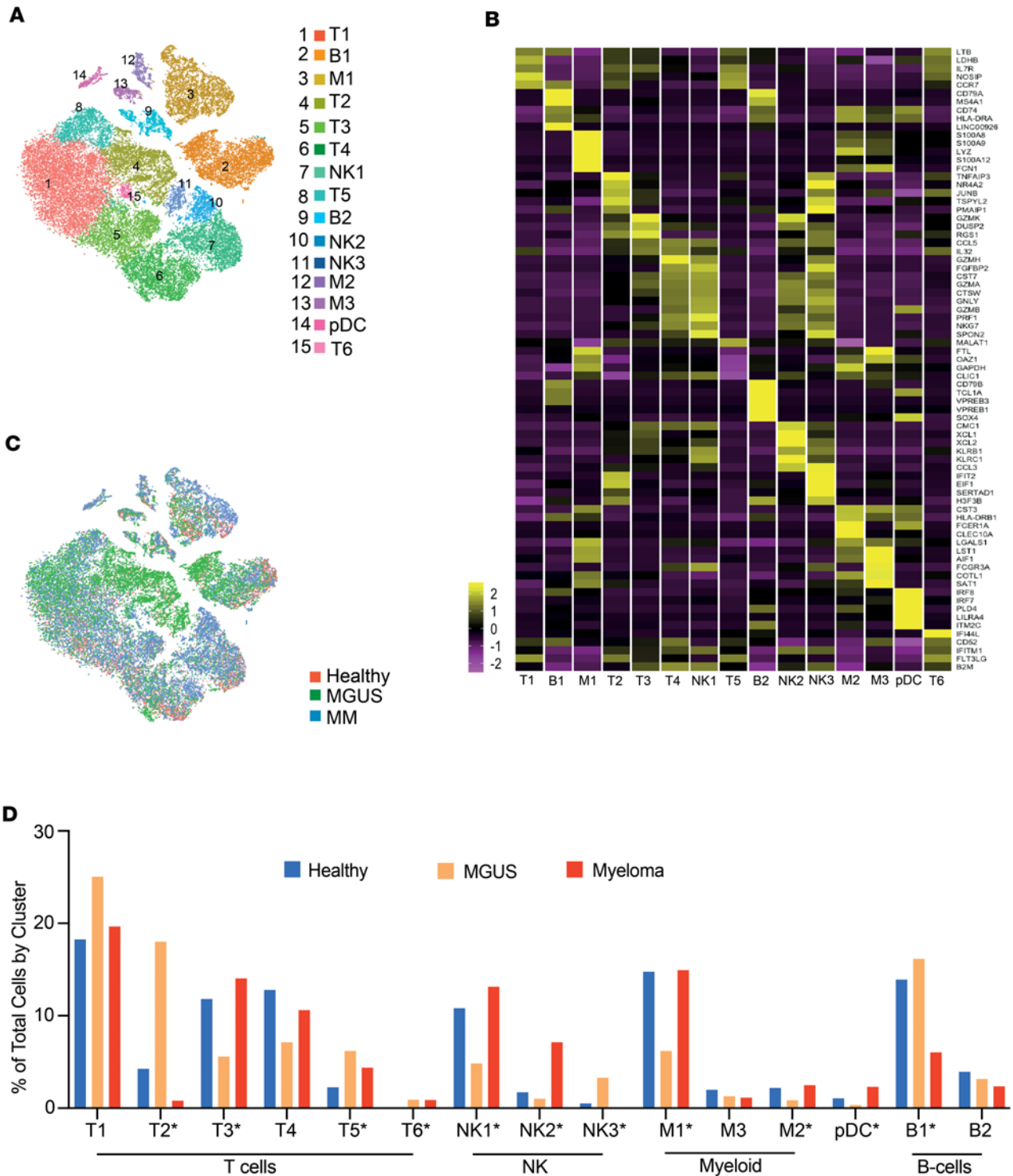
Figure 3. scRNA–Seq to characterize 42,606 bone marrow mononuclear immune cells from 33 samples (8 healthy donor, 14 MGUS, and 11 myeloma). (**A**) t-Distributed stochastic neighbor embedding (t-SNE) plot with 15 distinct cell populations determined by k-nearest neighbor unsupervised clustering. (**B**) Heatmap of zero-centered average gene expression of highly differentially expressed genes (selected by most extreme P value, Wilcoxon' rank-sum test) for each cluster identified in **A** compared with all other clusters. (**C**) t-SNE plot distinguishing cells by disease state. (**D**) Cells in each cluster as a percentage of total cells by disease state (*$P < 0.005$, χ^2 test).
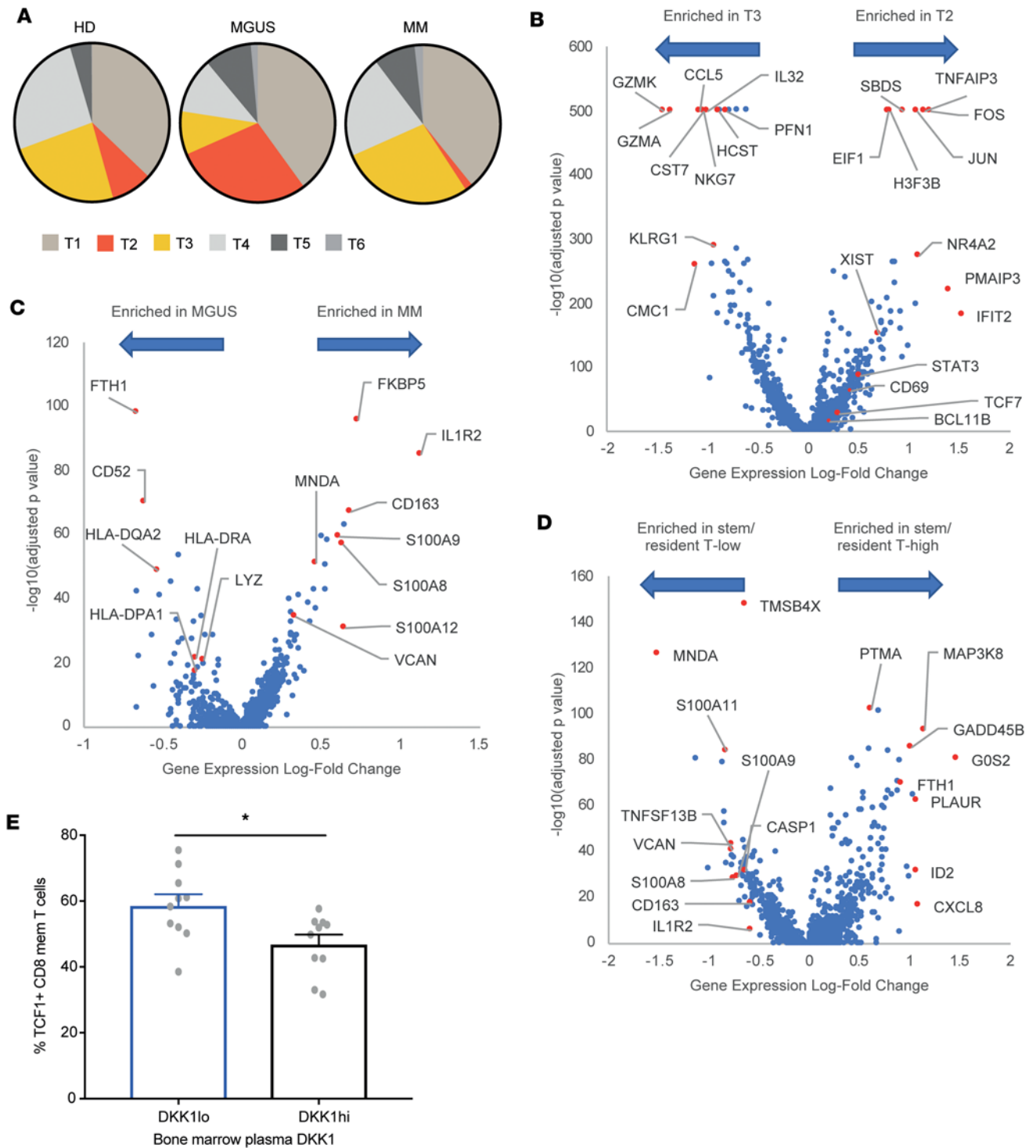
Figure 4. Characterization of gene expression differences in T cell and myeloid populations from scRNA-Seq. (**A**) T cells in each cluster as a percentage of total T cells. T2 cluster is enriched in MGUS (χ^2 $P < 0.0001$), and T3 cluster is enriched in MM (χ^2 $P < 0.0001$). (**B**) Volcano plot of differential gene expression between clusters T2 and T3. (**C**) Volcano plot of differential gene expression in myeloid cells between myeloma and MGUS. (**D**) Volcano plot of myeloid differential gene expression between samples with higher-than-mean population of cluster T2 stem-like/resident T cells and samples with lower-than-mean population of cluster T2 T cells. (**E**) DKK1 was measured in the plasma of MGUS and MM patients. Percentage of CD8+ memory cells that are TCF1+ in patients with DKK1 levels below median (DKK1lo: $n = 10$) and patients with DKK1 levels above median in the group (DKK1hi: $n = 10$). Bar graph shows mean ± SEM. *$P < 0.05$.

try data also suggested. Although T3 cluster is present in both healthy donors and patents with MM, the T3 cluster in MM revealed enrichment of PRDM1 (as a marker of exhaustion), Fos, and CCL4 (as a marker of activation) and downregulation of granulysin and lysozyme (as a marker of dysfunction) (Supplemental Figure 7). Taken together with the mass cytometry data (Figure 1), these studies show that T cells in MGUS are enriched for stem-like memory T cells, overlapping in part with a quiescent tissue-resident phenotype, while T cells in MM show greater expression of lytic genes and senescence markers.

Myeloid cells comprised 3 distinct clusters that correlated with monocytes (M1 cluster), as well as previously described CD1c+ or CD1c− dendritic cell clusters (M2 and M3 clusters) (17). Analysis of differentially expressed genes within myeloid clusters revealed reduced transcripts of HLA-DR in MM, consistent with a less activated phenotype and consistent with the mass cytometry data showing lower CD86 as a marker of reduced activation in MM myeloid cells (Figure 4C). Genes increased in MM myeloid cells also included several genes with possible implications for immunosuppressive properties (such as IL1R2 and calcium-binding proteins S100A8, S100A9, and S100A12), as well as other genes (e.g., versican) previously implicated in this role (18). GSEA of differentially expressed genes identified dendritic cell (DC) activation as a pathway altered in these cells, supporting a role for altered antigen presentation (Supplemental Figure 8). Cells from healthy donors and patients with MM in the M1 cluster were located somewhat differently in the t-SNE plot (Figure 3C). Top differentially expressed genes of cells in this cluster between healthy donors and patients with MM also supported altered myeloid polarization with a more immune-suppressive phenotype of myeloid cells in MM (Supplemental Figure 9).

To explore the link between T cell and myeloid changes, we examined the genomic profiles of myeloid cells from patients with a higher proportion of cells in T2 cluster. Myeloid cells from these patients revealed a distinct genomic profile consistent with an enrichment for genes associated with TLR-mediated DC activation on GSEA (Figure 4D and Supplemental Figure 10). Because TCF1 expression is known to be regulated by WNT signaling, we hypothesized that the depletion of TCF1+ cells may be related to increase in WNT inhibitor Dickkopf-1 previously described in MM (19). Consistent with this possibility, patients with elevated levels of Dickkopf-1 (DKK1) in the bone marrow plasma had reduced levels of TCF1+ memory T cells (Figure 4E).

Discussion

These data illustrate several changes in the immune landscape in MGUS and MM. The data show progressive increase in terminal effector T cells with progressive malignancy. However, the finding that terminal effector T cells were increased even in MGUS suggests that alterations in T cell differentiation originate early in carcinogenesis during premalignancy.

An important and potentially novel aspect of this paper is the finding that memory T cells in the bone marrow in MGUS are enriched for TCF1hi memory T cells that bear a resemblance to stem-like T cells (20). TCF1hi cells have to date been best studied in the context of models of chronic viral infections, wherein recent studies have illustrated their importance in preventing attrition of exhausted T cells and thereby maintaining long-term protective immunity (11, 12, 21). TCF1-expressing cells have also been recently identified in human cancer tissue and were linked to outcomes following checkpoint blockade in a small cohort (13, 22). To our knowledge, these are the first studies to identify specific enrichment of these cells in the tumor microenvironment in a human premalignancy. It is now well established that many of the mutations/neoantigens found in cancer that serve as critical targets of tumor immunity originate during the premalignant phase, particularly in MM (1, 2). Therefore, the observed enrichment and persistence of these cells in MGUS may be key to maintaining tumor immunity during the MGUS phase; loss of TCF1+ memory T cells in MM may lead to inability to maintain protective immunity over time and loss of immune surveillance. Although the cells identified in our studies bear a general resemblance to phenotypes observed in murine models of chronic viral infection, we and others (22) have not detected the expression of CXCR5 on these cells in the tumor tissue. Together, these data suggest that a hierarchy of exhausted clones wherein a small subset of stem-like cells prevent clonal attrition is already evident at the premalignant stage.

In recent studies, we and others have shown an important role for tissue-resident memory in protective tumor immunity (16, 23, 24). Similar cells were also identified in the human bone marrow and exhibited a quiescent phenotype with enrichment of transcription factors such as NR4A1 and NR4A2 that have been implicated in inhibiting T cell differentiation and effector function (15, 25, 26). Our data show that the T cell cluster enriched in MGUS shows features of both stem-like and tissue-resident memory, suggesting an overlap between these features of tumor-infiltrating T cells.

An important change in the MM tumor microenvironment relates to phenotype and gene expression in myeloid cells. Prior studies have shown that myeloid cells play an important role in regulating the growth of tumor cells (27, 28). The altered phenotype of tumor-infiltrating myeloid cells, including reduced expression of CD86, CD155, and c-KIT and increased PD-L1, supports an immune-suppressive phenotype. These data, therefore, support prior studies showing enrichment of myeloid cells in MM, including their protumor effects (18). Reduced expression of Fas in MM myeloid cells is of interest because Fas/FasL interactions play a major role in regulating myeloid cell kinetics, as illustrated by increased myeloid progenitors in mice with mutated Fas/FasL (29), and may contribute to their enrichment in MM.

In addition to changes in T cells, we observed changes in innate cells, with an increase in NK cells. NK cells in MM, however, revealed some functional alterations, such as decline in NKG2D. Therefore, alterations in innate lymphocytes appear to be an early feature in the evolution of gammopathies, which is consistent with prior studies (5, 30). Recent studies suggest that innate cells may be targets for immunomodulatory drugs currently being explored for prevention of myeloma (5).

The enrichment of stem-like and resident T cells in the MGUS marrow that we observed may be affected by local signals in the tumor bed. Prior studies have shown that local interactions with antigen-presenting cells in situ may be critical for tissue retention of murine tissue-resident memory T cells (31, 32). Consistent with this, we observed that enrichment of stem-like/resident T cells correlated with distinct genomic features of myeloid cells indicative of TLR-mediated activation. Further studies are needed to dissect the signals needed for retention and persistence of these cells in the bone marrow. Some of the signals that regulate these cells may also be derived from tumors themselves. For example, because TCF1 expression may depend on WNT signaling, WNT inhibitor DKK1, known to be increased in MM (19), may also contribute to the depletion of TCF1-expressing cells in MM. This hypothesis needs further study but is supported by the inverse correlation between DKK1 levels in the marrow and TCF1-expressing cells.

In summary, these studies use complementary high-content single-cell methods to gain novel insights into early changes in the immune microenvironment in MGUS/MM, with potential implications for immune therapy and prevention of MM. They illustrate early and complex alterations in the immune landscape in MGUS, including both innate and adaptive immune cells (Supplemental Figure 11). These data have several implications for immune-based approaches in MM. The presence of stem-like and resident T cells in tumor tissues has recently been linked to responsiveness to checkpoint blockade (22, 33). Depletion of stem-like and resident T cells and predominant accumulation of Ttes in MM may therefore contribute to the lack of tumor regression following PD-1 blockade in MM (34) and may also limit the durability of responses following T cell redirection therapies. The finding that this increase in Ttes begins presymptomatically suggests the need to investigate even earlier stages (e.g., pre-MGUS) (1) to better understand the origins of altered T cell differentiation programs. Further studies in larger cohorts are needed to test whether the loss of stem-like/resident T cells is predictive of the risk of progression to clinical MM or durability of immune therapies and whether preemptive interventions before such depletion might be most effective at achieving durable remissions. Alternatively, strategies that lead to an increase in the stem-like and marrow-resident pool may be effective in delaying both attrition of T cell response in MGUS and its evolution to clinical MM and may enhance the potential of durable remissions by engaging the immune system.

Methods

Patients and samples. Bone marrow samples were obtained from 26 patients with MGUS/MM following receipt of patients' informed consent approved by the institutional review board. Mononuclear cells were isolated by density gradient centrifugation. Bone marrow specimens from 12 healthy donors were purchased from All Cells Inc. Cells were cryopreserved in 90% FBS and 10% DMSO for long-term storage in liquid nitrogen.

Mass cytometry. Thawed bone marrow suspensions were stained with a 39- and 37-marker panel using metal-conjugated antibodies according to manufacturer-suggested concentrations (Fluidigm). Data on specific antibodies/clones are provided in Supplemental Table 2. Cells were fixed, permeabilized, and washed in accordance with the manufacturer's cell surface and nuclear antigen staining protocol (Fluidigm). After antibody staining, cells were incubated with intercalation solution, mixed with EQ Four Element Calibration Beads (catalog 201078), and acquired with a Helios mass cytometer (all from Fluidigm). Gating and data analysis were performed using Cytobank (https://www.cytobank.org/). Viable cells and doublets were excluded using cisplatin intercalator and DNA content with the iridium intercalator.

scRNA-Seq and data analysis. Bone marrow mononuclear cells were thawed and flow sorted to obtain live cells (healthy donor $n = 8$, and MGUS $n = 14$) and CD138⁻ live cells (MM $n = 11$). Barcoded libraries were prepared using the manufacturer's (10× Genomics) protocol and sequenced with Illumina HiSeq. Reads were aligned, filtered, deduplicated, and converted into a digital count matrix using Cell Ranger 1.2 (10× Genomics). Additional quality control and data analysis were performed using Seurat (35). Cells with fewer than 200 unique sequenced genes or more than 10% mitochondrial genes were removed, and cells with more than 7000 unique sequenced genes or more than 70,000 unique molecular identifiers were removed to exclude potential doublets. Genes with the greatest dispersion in expression across cells were used in principal component analysis. Identified principal components were used for k-nearest neighbor unsupervised clustering with adjustment by the Jaccard similarity, and data were visualized using t-SNE. Differentially expressed genes defining clusters were manually inspected to determine cluster identity. Pathway analysis of differentially expressed genes in T or myeloid cells was performed using GSEA software from the Broad Institute.

Statistics. Statistical analysis of mass cytometry data was performed using 2D graphing and statistics software GraphPad Prism. Nonparametric Mann-Whitney (for comparing 2 groups) and Kruskal-Wallis (for comparing 3 groups) tests with a significance threshold of $P < 0.05$ were used to compare different cohorts. Wilcoxon's rank-sum test with a significance threshold of $P < 0.05$ after Bonferroni's correction was used to identify differentially expressed genes between clusters and disease states in the scRNA-Seq data. We used χ^2 with a significance threshold of $P < 0.005$ to identify clusters with differential composition by disease state. Data in bar graphs were plotted as mean ± SEM.

Study approval. All studies involving human subjects were approved by institutional review boards at Yale and Emory University.

Author contributions

JKB designed and performed experiments, analyzed data, and wrote the manuscript. SMM analyzed data and wrote the manuscript. DBD, MS, and KP performed experiments and analyzed data. AKN, NN, TLP, NB, JLK, CCH, LHB, and SL performed clinical research and data analysis. MLK supervised data analysis. MVD and KMD designed and supervised research, analyzed data, and wrote the manuscript. All authors reviewed and edited the final manuscript.

Acknowledgments

Address correspondence to: Madhav V. Dhodapkar or Kavita M. Dhodapkar, 1760 Haygood Drive, Atlanta, Georgia 30322, USA. Phone: 404.778.1900; Email: madhav.v.dhodapkar@emory.edu (MVD). Phone: 404.778.1900; Email: Kavita.dhodapkar@emory.edu (KMD).

1. Dhodapkar MV. MGUS to myeloma: a mysterious gammopathy of underexplored significance. *Blood*. 2016;128(23):2599–2606.
2. Zhao S, et al. Serial exome analysis of disease progression in premalignant gammopathies. *Leukemia*. 2014;28(7):1548–1552.
3. Dhodapkar MV, Krasovsky J, Osman K, Geller MD. Vigorous premalignancy-specific effector T cell response in the bone marrow of patients with monoclonal gammopathy. *J Exp Med*. 2003;198(11):1753–1757.
4. Spisek R, et al. Frequent and specific immunity to the embryonal stem cell-associated antigen SOX2 in patients with monoclonal gammopathy. *J Exp Med*. 2007;204(4):831–840.
5. Kini Bailur J, et al. Changes in bone marrow innate lymphoid cell subsets in monoclonal gammopathy: target for IMiD therapy. *Blood Adv*. 2017;1(25):2343–2347.
6. Dhodapkar MV, Krasovsky J, Olson K. T cells from the tumor microenvironment of patients with progressive myeloma can generate strong, tumor-specific cytolytic responses to autologous, tumor-loaded dendritic cells. *Proc Natl Acad Sci U S A*. 2002;99(20):13009–13013.
7. Noonan K, et al. Activated marrow-infiltrating lymphocytes effectively target plasma cells and their clonogenic precursors. *Cancer Res*. 2005;65(5):2026–2034.
8. Noonan KA, et al. Adoptive transfer of activated marrow-infiltrating lymphocytes induces measurable antitumor immunity in the bone marrow in multiple myeloma. *Sci Transl Med*. 2015;7(288):288ra78.
9. Dhodapkar MV, et al. Prospective analysis of antigen-specific immunity, stem-cell antigens, and immune checkpoints in monoclonal gammopathy. *Blood*. 2015;126(22):2475–2478.
10. Das R, et al. Microenvironment-dependent growth of preneoplastic and malignant plasma cells in humanized mice. *Nat Med*. 2016;22(11):1351–1357.

11. Im SJ, et al. Defining CD8+ T cells that provide the proliferative burst after PD-1 therapy. *Nature*. 2016;537(7620):417–421.

12. Snell LM, et al. CD8+ T cell priming in established chronic viral infection preferentially directs differentiation of memory-like cells for sustained immunity. *Immunity*. 2018;49(4):678–694.e5.

13. Brummelman J, et al. High-dimensional single cell analysis identifies stem-like cytotoxic CD8. *J Exp Med*. 2018;215(10):2520–2535.

14. Kratchmarov R, Magun AM, Reiner SL. TCF1 expression marks self-renewing human CD8. *Blood Adv*. 2018;2(14):1685–1690.

15. Boddupalli CS, et al. ABC transporters and NR4A1 identify a quiescent subset of tissue-resident memory T cells. *J Clin Invest*. 2016;126(10):3905–3916.

16. Boddupalli CS, et al. Interlesional diversity of T cell receptors in melanoma with immune checkpoints enriched in tissue-resident memory T cells. *JCI Insight*. 2016;1(21):e88955.

17. Villani AC, et al. Single-cell RNA-seq reveals new types of human blood dendritic cells, monocytes, and progenitors. *Science*. 2017;356(6335):eaah4573.

18. Asimakopoulos F, Hope C, Johnson MG, Pagenkopf A, Gromek K, Nagel B. Extracellular matrix and the myeloid-in-myeloma compartment: balancing tolerogenic and immunogenic inflammation in the myeloma niche. *J Leukoc Biol*. 2017;102(2):265–275.

19. Tian E, et al. The role of the Wnt-signaling antagonist DKK1 in the development of osteolytic lesions in multiple myeloma. *N Engl J Med*. 2003;349(26):2483–2494.

20. Hashimoto M, et al. CD8 T cell exhaustion in chronic infection and cancer: opportunities for interventions. *Annu Rev Med*. 2018;69:301–318.

21. Wu T, et al. The TCF1-Bcl6 axis counteracts type I interferon to repress exhaustion and maintain T cell stemness. *Sci Immunol*. 2016;1(6):eaai8593.

22. Sade-Feldman M, et al. Defining T cell states associated with response to checkpoint immunotherapy in melanoma. *Cell*. 2018;175(4):998–1013.e20.

23. Amsen D, van Gisbergen KPJM, Hombrink P, van Lier RAW. Tissue-resident memory T cells at the center of immunity to solid tumors. *Nat Immunol*. 2018;19(6):538–546.

24. Ganesan AP, et al. Tissue-resident memory features are linked to the magnitude of cytotoxic T cell responses in human lung cancer. *Nat Immunol*. 2017;18(8):940–950.

25. Milner JJ, et al. Runx3 programs CD8+ T cell residency in non-lymphoid tissues and tumours. *Nature*. 2017;552(7684):253–257.

26. Milner JJ, Goldrath AW. Transcriptional programming of tissue-resident memory CD8. *Curr Opin Immunol*. 2018;51:162–169.

27. Zheng Y, et al. Macrophages are an abundant component of myeloma microenvironment and protect myeloma cells from chemotherapy drug-induced apoptosis. *Blood*. 2009;114(17):3625–3628.

28. Kukreja A, et al. Enhancement of clonogenicity of human multiple myeloma by dendritic cells. *J Exp Med*. 2006;203(8):1859–1865.

29. Alenzi FQ, et al. A role for the Fas/Fas ligand apoptotic pathway in regulating myeloid progenitor cell kinetics. *Exp Hematol*. 2002;30(12):1428–1435.

30. Guillerey C, Nakamura K, Vuckovic S, Hill GR, Smyth MJ. Immune responses in multiple myeloma: role of the natural immune surveillance and potential of immunotherapies. *Cell Mol Life Sci*. 2016;73(8):1569–1589.

31. Park SL, et al. Local proliferation maintains a stable pool of tissue-resident memory T cells after antiviral recall responses. *Nat Immunol*. 2018;19(2):183–191.

32. Shin H, Kumamoto Y, Gopinath S, Iwasaki A. CD301b+ dendritic cells stimulate tissue-resident memory CD8+ T cells to protect against genital HSV-2. *Nat Commun*. 2016;7:13346.

33. Dhodapkar KM. Role of tissue-resident memory in intra-tumor heterogeneity and response to immune checkpoint blockade. *Front Immunol*. 2018;9:1655.

34. Lesokhin AM, et al. Nivolumab in patients with relapsed or refractory hematologic malignancy: preliminary results of a phase Ib study. *J Clin Oncol*. 2016;34(23):2698–2704.

35. Satija R, Farrell JA, Gennert D, Schier AF, Regev A. Spatial reconstruction of single-cell gene expression data. *Nat Biotechnol*. 2015;33(5):495–502.